Clin Oral Invest (2013) 17:139–146
DOI 10.1007/s00784-012-0680-x

ORIGINAL ARTICLE

The color change in artificial white spot lesions measured using a spectroradiometer

Younju Kim · Ho-Hyun Son · Keewook Yi · Hae-Young Kim · Jinsoo Ahn · Juhea Chang

Received: 15 September 2011 / Accepted: 16 January 2012 / Published online: 27 January 2012

Abstract
Objectives The purpose of this study was to determine the color of white spot lesions.
Materials and methods Human premolars were subjected to a pH cycling to produce artificial caries lesions and classified into groups (n=10/group): group 1, immersion in deionized water; group 2, pH cycling without fluoride (F) application; group 3, pH cycling with immersion in 1,000 ppm NaF solution; and group 4, pH cycling with immersion in 5,000 ppm NaF solution. CIE $L^*a^*b^*$ color parameters of the tooth were determined using a spectroradiometer at baseline, after demineralization and after pH cycling. The extent of demineralization was evaluated by scanning electron microscopy (SEM) and electron microprobe analysis (EPMA).
Results Significant degrees of color change (ΔE^*) were observed after demineralization ($p<0.05$). The changes were mainly due to an increase in lightness (L^*) and a decrease in yellowness (b^*). F application induced a significantly large ΔE^* in group 4 ($p<0.05$). The color reversal after remineralization was mostly due to the recovery of L^*. SEM and EPMA verified that net mineral gains occurred in the subsurface lesions.
Conclusions The initially white appearance of enamel caries was a result of changes of L^* and b^*. F treatment partially restored the color of white spot lesions.
Clinical relevance F-driven remineralization induced both mineral gains and esthetic enhancement of artificially produced enamel white spot lesions. The increase of L^* and the decrease of b^* contributed to the color changes.

Keywords Color · Fluoride · Remineralization · Spectroradiometer · White spot lesion

Y. Kim · H.-H. Son
Department of Conservative Dentistry and Dental Research Institute, School of Dentistry, Seoul National University, Seoul, South Korea

K. Yi
Geochronology Team, Korea Basic Science Institute, Daejeon, South Korea

H.-Y. Kim
Department of Dental Laboratory Science and Engineering, College of Health Science, Korea University, Seoul, South Korea

J. Ahn
Department of Dental Biomaterials Science, Dental Research Institute, School of Dentistry, Seoul National University, Seoul, South Korea

J. Chang (✉)
Clinic for Persons with Disabilities, Seoul National University Dental Hospital, Dental Research Institute, School of Dentistry, Seoul National University,
101 Daehak-no, Jongno-gu,
Seoul 110-768, South Korea
e-mail: juhchang@snu.ac.kr

Introduction

Initial caries lesions induce a loss of mineral while maintaining an intact surface layer. The increased porosity within the subsurface crystalline structure enhances optical scattering, providing a visually discernable white spot lesion [1]. A white spot lesion with a reasonably hardened surface layer maintains its mechanical and chemical properties in the oral environment and does not require any immediate restorative treatment. However, the whiteness of the enamel surface often leads to esthetic concerns for patients, necessitating minimally invasive interventions, such as tooth whitening, microabrasion, or resin infiltration [2]. The main goal for the

treatment of white spot lesions is not only to prevent further demineralization but also to lessen the whiteness of the initial lesion to resemble the color of the adjacent sound tissue.

The color statuses of natural teeth and esthetic restorative materials have been extensively investigated based on the color measurement systems such as CIE $L^*a^*b^*$ color coordinates. The CIE $L^*a^*b^*$ system is composed of three components: L^* represents the lightness, while a^* and b^* denote the coordinates on the red–green and yellow–blue color axes, respectively [3]. The tristimulus values in the CIE $L^*a^*b^*$ space are closely related to the human visual response, which is sensitive to three different wavelength ranges (red, green, and blue) between 360 and 780 nm. Until now, only a few studies have been conducted on the color determination of demineralized tooth structure. CIE $L^*a^*b^*$ values obtained from photographic images of carious dentin showed that the L^* and a^* values were related to caries activity [4].

A recent study using a spectrophotometer showed that resin infiltration and fluoride (F) therapy influenced the lightness (L^*) of demineralized bovine enamel [1].

Conventional reflectance measurements taken using a spectrophotometer or a colorimeter are subject to the edge-loss effect, i.e., the illuminating light penetrates into the translucent material and travels to the edges, some of which is lost without reflection [5]. Therefore, color measurement systems without the edge-loss effect are required for the evaluation of tooth specimens given the wide range of translucency of enamel and dentin [6]. In non-contact measurement devices, such as spectroradiometers, there is no aperture between the external light source and the object. Thus, shadows cast on the specimen can be avoided without the interference of light intensity during observation [7].

Considering that the aforementioned treatment modalities for white spot lesions involve minimal and microinvasive approaches, the repair of porous structures via remineralization can be an ideally non-invasive restoration. With the F-driven deposition of calcium (Ca) and phosphate (P) ions, crystal repair in the subsurface lesion decreases the scattering effect of the enamel, which affects the perception of the overall tooth color [8, 9]. There are some clinical studies showing that the use of topical F contributed to the regression or disappearance of white spot lesions [10, 11]. However, the clinically favorable outcome may be related to the mechanical removal of the surface-softened tissue by abrading motion of toothbrush and paste [12].

In this in vitro study, we produced initial caries lesions with a preserved surface layer and induced subsurface remineralization via F application. Also, the extents of demineralization and remineralization of the lesion area was determined using scanning electron microscopy (SEM) and elemental analysis. The aims of this study were (1) to identify the CIE $L^*a^*b^*$ values of white spot lesions using a spectroradiometer and (2) to determine the effect of F treatment on the CIE $L^*a^*b^*$ values of white spot lesions. The null hypothesis was that there was no difference in CIE $L^*a^*b^*$ values of white spot lesions between before and after F treatment.

Materials and methods

Specimen preparation

This study was approved by the Institutional Review Board at Seoul National University Dental Hospital (IRB No. CRI09019). Ten human upper premolars extracted during orthodontic treatment were used within 6 months of extraction. The teeth were disinfected in 0.5% chloramine-T for a week and stored in distilled water at 4°C. The teeth were inspected under a ×10 stereomicroscope (Jaemyung Ind., Seoul, Korea) to ensure that they were free of white spot lesions or other defects. The roots of the teeth were removed at the cementoenamel junction with a low-speed diamond saw (Isomet, Buehler, Lake Bluff, IL, USA). The crown part was sectioned mesiodistally and buccolingually into four parts. Each quarter of the crown was ground on the dentin side, leaving a 2-mm-thick dentin layer. The sections were then embedded using hot-melt adhesive (polyvinyl alcohol) with a 2×4-mm window on the enamel surface left exposed. To produce a white spot lesion, each specimen was immersed in 2.5 ml of demineralizing solution (1.5 mM $CaCl_2$, 0.9 mM KH_2PO_4, 50 mM acetate buffer, pH 4.8), followed by immersion in 2.5 ml of remineralizing solution (1.5 mM $CaCl_2$, 0.9 mM KH_2PO_4, 20 mM HEPES (4-(2-hydroxyethyl)-1-piperazineethanesulfonic acid), pH 7.0) [13] at 4°C with a daily change of solution (Table 1). Specimens were rinsed using deionized water for 20 s at every change. After white spot lesion formation, each of the four specimens from the same tooth was randomly allocated into one of the following four groups (n=10/group):

Group 1: No treatment (control)
Group 2: pH cycling without fluoride application
Group 3: pH cycling with immersion in 1,000 ppm NaF solution
Group 4: pH cycling with immersion in 5,000 ppm NaF solution

CIE $L^*a^*b^*$ color measurement

The color of the enamel surface was measured at baseline, after the formation of white spot lesion, and after F application with pH cycling. For the color measurement,

Table 1 Treatment sequences for the experimental groups

Group (treatment regimen)	Treatment sequences	
	White spot lesion formation	Remineralization
1 (no treatment)	First pH cycling (1 time): demineralization (96 h)+remineralization (24 h)	Immersion in water (7 days)
2 (only pH cycling)		pH cycling[a] (7 days)
3 (pH cycling+1,000 ppm NaF treatment)	Second pH cycling (7 times): demineralization (3 h)+remineralization (20 h)	pH cycling[a] (7 days) with immersion in 1,000 ppm NaF (1 h)
4 (pH cycling+5,000 ppm NaF treatment)		pH cycling[a] (7 days) with immersion in 5,000 ppm NaF (1 h)

[a]A daily pH cycling comprised of 3 h demineralization and 20 h remineralization

specimens were retrieved from storage solution (distilled water), dried with blotting paper, and immediately placed in a light booth (Color Sense II; Sungjin Hitech, Gyeonggi-Do, Korea) with Munsell N7 neutral gray walls and floor (Fig. 1). A spectroradiometer (PR-670; SpectraScan, Photo Research, Chatsworth, CA, USA) equipped with a Macro-Spectar MS-75 lens (Photo Research) was fixed on a tripod at a distance of 355 mm from the measured object and with a measurement area of 2.63 mm in diameter, providing an optical configuration of 2° observation to the object [14]. Four D65 simulating tubes (F20T12/65; GretagMacbeth, Research Triangle Park, NC, USA), having a correlated color temperature of 6,500 K and a color rendering index (CRI) of 91, were used as a light source. The tubes were bi-directionally fixed with a 45° illumination angle at a distance of 20 cm from the measured object. External light was excluded by covering all the equipments with a lightproof cover. The positioning of the lens towards the surface of the specimen was kept constant to ensure the standardized measurement throughout the experiment. Spectral reflectance was obtained from 380 to 780 nm with a 2-nm interval (Spectrawin 2.0, Photo Research) and subsequently converted to the CIE L^*, a^*, and b^* values. Color difference (ΔE^*) was calculated by the equation: $(\Delta E^*)=[(\Delta L^*)^2+(\Delta a^*)^2+(\Delta b^*)^2]^{1/2}$. Every measurement was performed after calibration made over white background and repeated three times.

SEM/electron microprobe analysis (EPMA)

Specimens were embedded in epoxy resin (Epofix, Struers, Glasgow, UK) and horizontally cross-sectioned along the midline. The cut surfaces were serially polished with 1,200, 2,400, and 4,000 grit aluminum oxide (Al_2O_3) abrasive papers, followed by 1 and 0.25 μm diamond, and 0.1 and 0.05 μm alumina polishing suspensions (Struers, Copenhagen, Denmark). The specimens were ultrasonically cleaned in deionized water for 10 min, dried for 72 h in a desiccator, and then sputter-coated with carbon. Demineralization bands on the cross-sectioned surfaces were identified using the phase contrast of backscattered electron imaging (BSI) mode of a SEM (JEOL JSM-6610LV, JEOL, Akishima, Japan). Two line analyses were performed perpendicular to the outer enamel surface at 0.3-μm-pixel intervals. The observation areas (superficial layer, demineralized layer, and inner sound enamel) were determined according to changes in Ca and P contents using an electron microprobe (JEOL JXA-8100, JEOL, Akishima, Japan). The operating conditions for the elemental analyses were 15 kV of accelerating voltage and 50 nA of beam current. A fluorapatite crystal (3.38% F) was used as a standard comparison for F.

Statistical analysis

The mean values (SD) of CIE L^*, a^*, and b^* between each of the following pairs of measurement points, baseline (BL) and caries formation (CA), CA and remineralization (RE), and RE and CA, were compared. ΔE^* obtained between each measurement point was compared among the four groups. Distribution of the data was examined using the Shapiro–Wilk test in prior to data analysis procedure considering the relatively small sample size. Assuming normal distribution of color differences ($p>0.05$), the analysis of

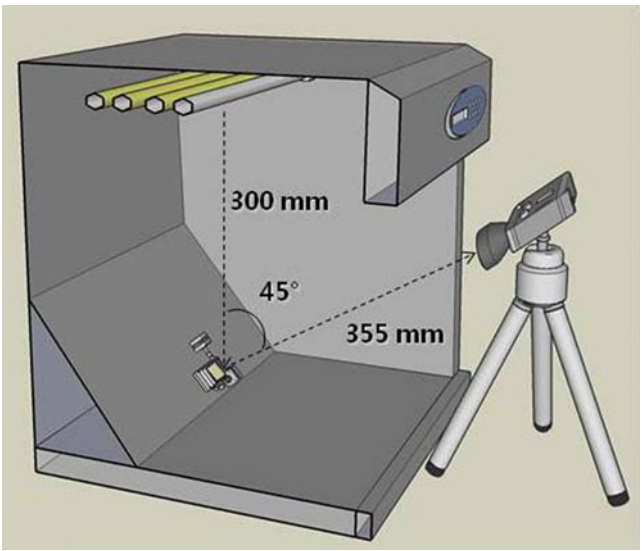

Fig. 1 Schematic of the spectroradiometer measurement set-up

variance (ANOVA) was performed with Tukey's post-hoc comparison.

Results

Figure 2 and Table 2 show the mean values of CIE L^*, a^*, and b^* at BL, CA, and RE. At BL, there was no significant difference in L^* (p=0.751), a^* (p=0.051), or b^* (p=0.502) among all the groups. At CA, an increase in L^*, meaning a change to a lighter color, was prominent with a mean increase ranging from 6.8 [standard deviation (SD) 3.3] to 8.4 (3.9) CIE units among all the groups. The mean a^* value decreased slightly by 0.7 (0.3) to 2.6 (1.2) CIE units, while the mean b^* value decreased moderately by 3.2 (3.1) to 7.8 (3.4) CIE units. The color difference between BL and CA, $\Delta E^*_{(BL–CA)}$, was not significantly different among all the groups (p>0.05). At RE, the mean L^* value changed by −4.2 (3.2) to 0.9 (2.2) CIE units among all the groups. The difference in the mean a^* value was limited between 0.1 (0.3) and 0.7 (0.3) CIE units. The difference in the mean b^* value was −2.0 (3.4) to 0.6 (1.6) CIE units. The color difference between CA and RE ($\Delta E^*_{(CA–RE)}$) in group 4 was significantly different from that in group 1 [6.1 (2.1) vs. 2.4 (2.2); p=0.001]. There were no differences in $\Delta E_{(CA–RE)}$* among groups 2, 3, and 4 (p>0.05). The color difference between RE and BL ($\Delta E^*_{(RE–BL)}$) in group 4 was significantly smaller than that in group 1 [6.2 (3.0) vs. 11.4 (3.3); p=0.019].

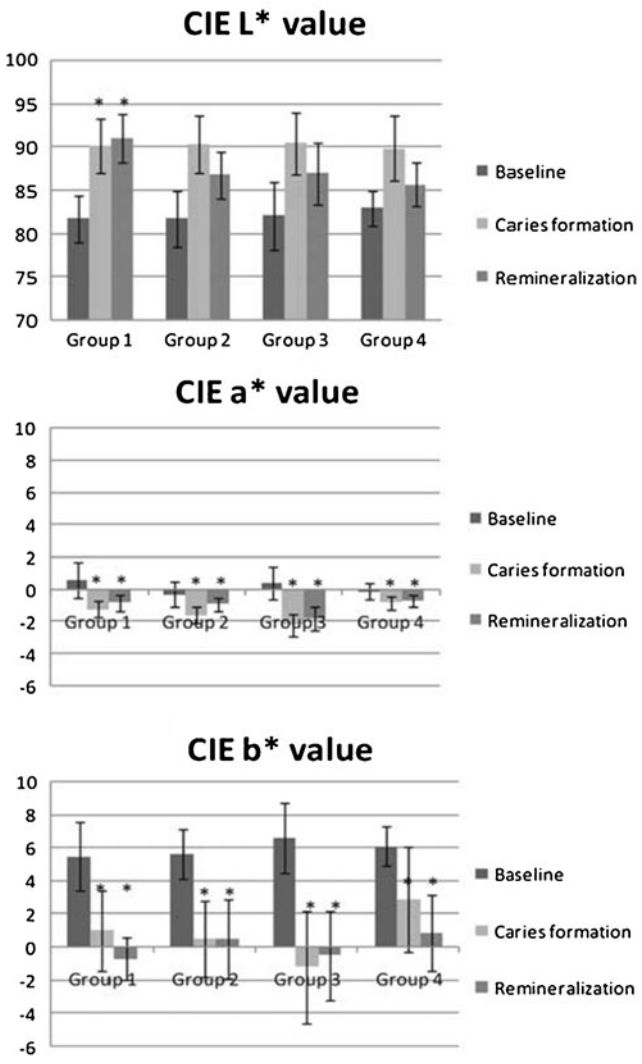

Fig. 2 CIE L^*, a^*, b^* values at baseline, after caries formation, and after remineralization

SEM revealed the formation of a subsurface demineralization area underneath a thinly preserved superficial layer (Fig. 3). Line analyses using electron microprobe analysis (EPMA) identified the individual distributions of Ca, P, and F, which made it possible to distinguish the demineralized layer from the inner sound enamel. The Ca and P levels dropped in the area that was represented by a dark band in the micrograph. Ca and P levels started to decrease after the first 10 to 15 μm and stayed low in the following subsurface area. The width of the subsurface lesion ranged from 40 to 50 μm.

Discussion

Color determination of a natural tooth involves non-homogeneous layers of the structure with curved surfaces, resulting in measurement variations according to specimen thickness, translucency, gloss, backing conditions, and surface irregularities [15, 16]. The perceived color of a tooth results from the reflection of incident light, in addition to the effect of scattered light within the enamel and dentin structures. Optical characterization of teeth has been widely used in the detection and quantification of caries lesions [10]. The enhanced scattering in the porous enamel acts as a barrier for the excitation light to reach the underlying sound tissues. Fluorescent light is also prevented from the layers below the lesion to reach the tooth surface. Based on this phenomenon, the quantification of enamel fluorescence has been a long-established diagnostic method in caries detection. However, color measurements are rarely conducted on enamel caries, although increased whiteness appearing in early lesions often causes concerns and requires restorative intervention. Our first aim was to determine the perceived appearance of demineralized enamel structure based on CIE L^*, a^*, and b^*, which are frequently used color parameters in esthetic restorative dentistry [3]. In this study, each quarter of a single tooth was allocated into one of four different groups, since the optical properties of a tooth can be affected by variations in substrate characteristics such as mineral density, crystal size, and prism orientation [8]. The enamel surface

Table 2 The difference in the mean values (SD) of CIE L^*, a^*, b^*, and ΔE^* between each of the following pairs of measurement points: baseline (BL) and caries formation (CA), CA and remineralization (RE), and RE and CA. Different superscript letters denote values that are significantly different from one another in each column ($p<0.05$)

Group (N=10/group)	Baseline (BL)			ΔE^* (BL-CA)	Caries formation (CA)			ΔE^* (CA-RE)	Remineralization (RE)			ΔE^* RE-BL)
	L^*	a^*	b^*		L^*	a^*	b^*		L^*	a^*	b^*	
1	81.7 (2.7)	0.6 (1.1)	5.5 (2.1)	10.1 (4.5)	90.2 (3.2)	−1.2 (0.5)	1.0 (2.4)	2.4 (2.2)^{a}	91.0 (2.8)	−0.8 (0.5)	−0.7 (1.3)	11.4 (3.3)^{a}
2	81.7 (3.3)	−0.3 (0.8)	5.6 (1.5)	10.3 (4.4)	90.4 (3.3)	−1.6 (0.5)	0.5 (2.3)	3.8 (1.4)^{a,b}	86.8 (2.7)	−0.9 (0.4)	0.5 (2.4)	7.7 (3.9)^{a,b}
3	82.1 (3.9)	0.4 (1.0)	6.6 (2.1)	12.0 (4.8)	90.5 (3.6)	−2.2 (0.7)	−1.2 (3.4)	3.9 (1.8)^{a,b}	87.0 (3.6)	−1.8 (0.7)	−0.5 (2.7)	9.3 (4.2)^{a,b}
4	83.0 (2.0)	−0.1 (0.5)	6.1 (1.2)	7.9 (3.7)	89.9 (3.7)	−0.8 (0.4)	2.9 (3.2)	6.1 (2.1)^{b}	85.7 (2.6)	−0.7 (0.4)	0.9 (2.3)	6.2 (3.0)^{b}
p value				0.248				0.001				0.019

was not ground in order to reflect the natural topography, maintained by a well-preserved superficial layer. Measurements could still be taken with a spectroradiometer, which is a non-contact appliance, while surface-flattened specimens were preferred for conventional contact measurement devices [6, 17]. The positioning of the specimen was carefully maintained at each measurement by coordinating indentation marks on the lateral sides of the specimen and the platform of the spectroradiometer. The whole surface of specimen is illuminated with a spectroradiometer, while a standardized area is in contact with a small-window aperture of a spectrophotometer. Hence, spectroradiometer-based color measurements more closely simulate color perception by human eyes and are less prone to color coordinates deviation, compared to other contact-measurement devices [18, 19]. In this study, the specimens had a standardized dentin backing thickness and were not significantly different with respect to baseline color ($p<0.05$). The mean L^* values ranged from 81.7 (2.7) to 83.0 (2.0) among all the groups. In the previous study using a spectroradiometer, the mean L^* value of human incisors was 82.23 (4.54), which was very similar to our results [20].

We intended to simulate a well-preserved enamel surface resembling a clinically long-lasting white spot lesion, although this in vitro experimental setting did not reflect adjoining biofilm, pH, food colorant, and metabolic byproducts which influence the optical properties of the early enamel caries [21]. SEM and EPMA showed that the superficial layer with a thickness of 10–20 μm had mineral contents equivalent to those of the underlying sound enamel (Fig. 3). The artificially formed white spot lesion resulted in a noticeable deviation in the values of L^* and b^*, but only minimal alteration in a^*, when compared to the baseline. These patterns of color change were similar to the outcomes of conventional tooth bleaching using peroxide-containing products [3]. Bleaching treatment usually results in an increase in lightness (L^*) and a decrease in yellowness (b^*). The color change in bleached teeth is known to be due not only to the removal of colorants but also to the enhancement of the inherent darkness of the tooth [22]. It is speculated that rapidly developed surface-softened enamel lesions can be adversely affected by chemically active peroxide radicals. There was one in vitro study which evaluated the bleaching effect on the enamel with artificial caries [23]. It was shown that 10% carbamide peroxide promoted an increase in mineral loss and surface morphological changes of carious enamel. In other study, bleaching agents even incorporated with F did not support further remineralization [24]. Hence, achieving esthetic enhancement of white spot lesions in addition to substantial reinforcement of the porous crystalline structure would be an entirely non-invasive protocol and an ideal treatment modality. The secondary aim of this study was to determine the potential of color reversal of white spot lesions through F-driven remineralization. Remineralization in caries management is not mineral precipitation onto enamel surfaces, but crystal repair that occurs in the subsurface lesion area [25]. In our study, this type of mineral gain was verified by elemental analysis combined with corresponding micrographs. In group 4 (5,000 ppm F), mineral deposition in the demineralized layer was shown to occur and approach the level seen in the inner sound enamel (Fig. 3d). Comparably, in group 3 (1,000 ppm), the mineral gain seemed not as substantial as in group 4 (Fig. 3c). With the external F concentration elevated, the driving force of F is exerted deep into the lesion, where increased surfaces of crystallite are available for F adsorption [26, 27]. In the previous study using EMPA, the bulk of F ions were incorporated into the body of the lesion matching the area that had the greatest increase in mineral density [25]. This was also observed in our study; however, the relatively low gradient of F in group 3 seemed to have reduced ion transport activity. Furthermore, the perfectly preserved surface layer might have hampered the incorporation of free ions into the subsurface area [28]. Group 2 was only subjected to pH cycling without additional F treatment. This group showed a slight sign of remineralization on elemental analysis (Fig. 3b). Even without F supplementation, the concentration gradient of Ca and P in the fluid environment possibly enabled the transportation of ions into the lesion area [29].

The extent of remineralization verified by SEM and EPMA were consistent with the degree of color change measured by the spectroradiometer. Group 4 showed the

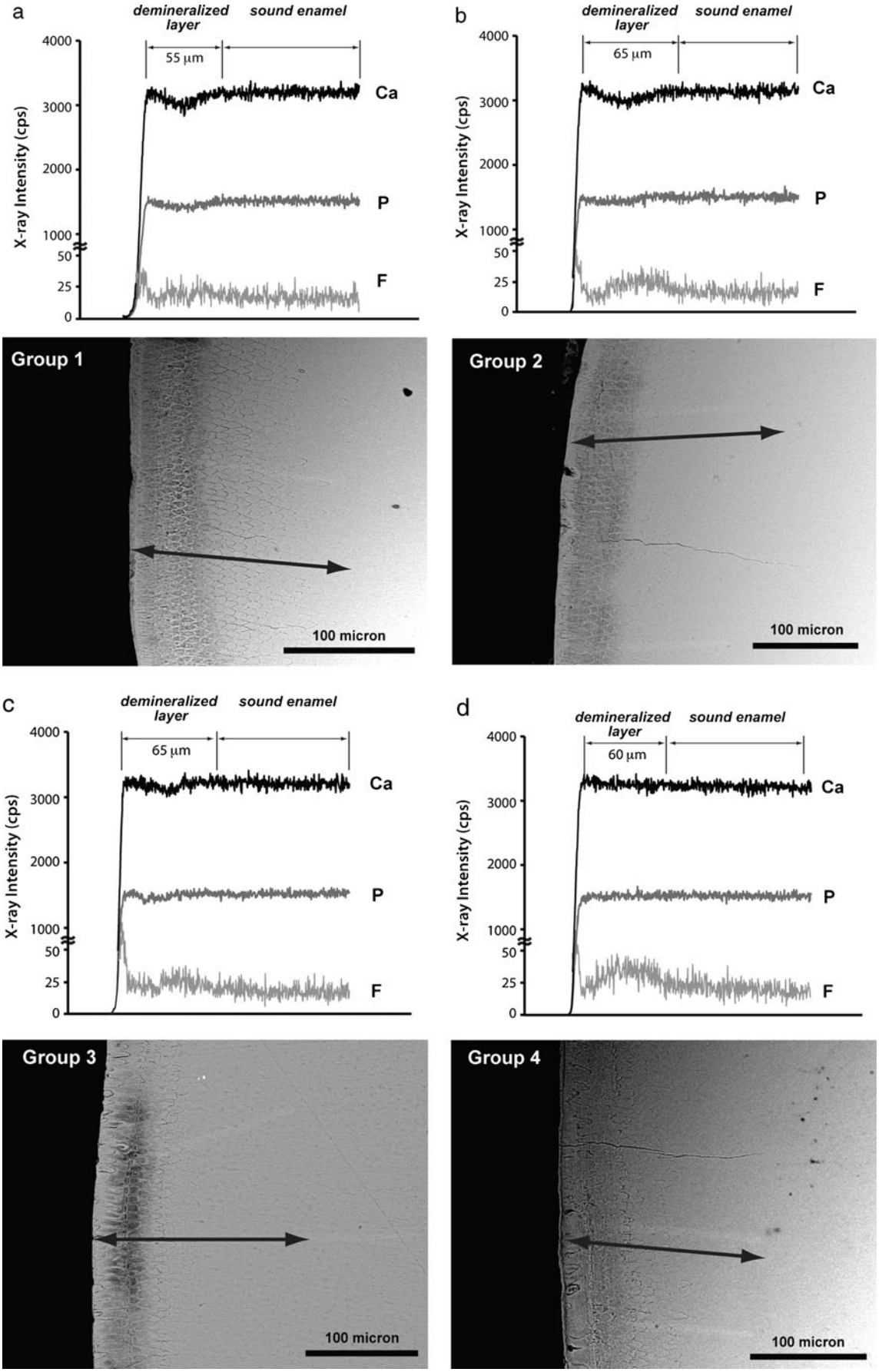
a
demineralized layer
sound enamel
55 µm
X-ray Intensity (cps)
4000
3000
2000
1000
50
25
0
Ca
P
F
b
demineralized layer
sound enamel
65 µm
Group 1
100 micron
Group 2
100 micron
c
demineralized layer
sound enamel
65 µm
d
demineralized layer
sound enamel
60 µm
Group 3
100 micron
Group 4
100 micron

◀ **Fig. 3** SEM images and EMPA graphs were compared for each experimental group (×600). Images were taken for each specimen originating from an identical tooth. Elemental analysis along the scan line illustrates the differentiated elemental composition (Ca, P, and F). **a** Group 1: a demineralization area underneath a thin superficial layer is represented by a *dark shadow*. Note that the Ca and P levels dropped in the demineralized layer. **b** Group 2: the demineralized layer exhibited similar features to that in group 1. Ca and P levels decreased in the demineralized layer. **c** Group 3: a slight sign of mineral deposition in the demineralized layer appeared. Ca and P levels remained with a decrease in the corresponding area. **d** Group 4: the demineralized layer was not easily recognizable due to the faded shadow in the image. EPMA showed the regained levels of Ca and P in the demineralized layer. The F level exceeded 25 units by X-ray intensity, which was noticeably higher than that in the other groups. The elevated amount of F abruptly decreased at the termination of the aforementioned area and leveled off in the sound enamel area

largest value of ΔE^* between CA and RE, and the value (6.1 units) exceeded the clinically discernable amount (2.6 units) [30]. Therefore, our null hypothesis was rejected. As shown in Fig. 3, increased lightness (ΔL^*) contributed to the majority of the color change (ΔE^*), while minimal changes in a^* and b^* were observed at RE. However, even in group 4, a clinically noticeable disparity in ΔE^* remained between BL and RE (6.2 units). During caries development, varying ionic composition of the fluid in a caries lesion allows for the reprecipitation of mineral phases different than those of the original structure [31, 32]. The repaired crystalline structure may contain a different directional arrangement, reflecting its altered optical properties [9]. It also may be that enlarged pore spaces have not been completely refilled, although elemental intensities of Ca and P were regained in the subsurface lesion [33]. It has been well established that previously demineralized enamel cannot be completely repaired even with transformed types of apatite [9, 25]. Our result may be related to the fact that long-existing white spot lesions remain inactive throughout several years, but show no detectable color change [34]. Future approaches may introduce the methodologies which enable to extend remineralization of subsurface lesions in a long-term period. Surface pre-treatment also need be considered for facilitation of ionic transportation. To restore physical appearance of natural tooth structure, substitution of the mineral-depleted porosities may be achieved by not only inorganic ions but also organic compound materials, which was demonstrated earlier in the resin infiltration technique [1, 2]. Based on the limitations of this in vitro study, the color of artificially produced initial caries was perceived as whiteness, which was a result of the changes in lightness (L^*) and yellowness–blueness (b^*) of the demineralized tooth structure. Remineralization promoted by the high concentration of F provided a noticeable change in the color of the tooth. However, the whiteness in the remineralized enamel still remained under the short-term F treatment, yielding a clinically discernable mismatch of color.

Conflicts of interest The authors declare that they have no conflicts of interest.

References

1. Torres CR, Borges AB, Torres LM, Gomes IS, de Oliveira RS (2010) Effect of caries infiltration technique and fluoride therapy on the colour masking of white spot lesions. J Dent. doi:10.1016/j.jdent.2010.12.004
2. Kielbassa AM, Muller J, Gernhardt CR (2009) Closing the gap between oral hygiene and minimally invasive dentistry: a review on the resin infiltration technique of incipient (proximal) enamel lesions. Quintessence Int 40:663–681
3. Joiner A, Hopkinson I, Deng Y, Westland S (2008) A review of tooth colour and whiteness. J Dent 36(Suppl 1):S2–S7
4. Iwami Y, Hayashi N, Takeshige F, Ebisu S (2008) Relationship between the color of carious dentin with varying lesion activity, and bacterial detection. J Dent 36:143–151
5. Johnston WM, Hesse NS, Davis BK, Seghi RR (1996) Analysis of edge-losses in reflectance measurements of pigmented maxillofacial elastomer. J Dent Res 75:752–760
6. Yu B, Ahn JS, Lee YK (2009) Measurement of translucency of tooth enamel and dentin. Acta Odontol Scand 67:57–64
7. Kim JC, Yu B, Lee YK (2008) Influence of surface layer removal of shade guide tabs on the measured color by spectrophotometer and spectroradiometer. J Dent 36:1061–1067
8. Ko CC, Tantbirojn D, Wang T, Douglas WH (2000) Optical scattering power for characterization of mineral loss. J Dent Res 79:1584–1589
9. Jones RS, Fried D (2006) Remineralization of enamel caries can decrease optical reflectivity. J Dent Res 85:804–808
10. Tranaeus S, Al-Khateeb S, Bjorkman S, Twetman S, Angmar-Mansson B (2001) Application of quantitative light-induced fluorescence to monitor incipient lesions in caries-active children. A comparative study of remineralisation by fluoride varnish and professional cleaning. Eur J Oral Sci 109:71–75
11. Du M, Cheng N, Tai B, Jiang H, Li J, Bian Z (2011) Randomized controlled trial on fluoride varnish application for treatment of white spot lesion after fixed orthodontic treatment. Clin Oral Investig. doi:10.1007/s00784-011-0520-4
12. Kielbassa AM, Gillmann L, Zantner C, Meyer-Lueckel H, Hellwig E, Schulte-Monting J (2005) Profilometric and microradiographic studies on the effects of toothpaste and acidic gel abrasivity on sound and demineralized bovine dental enamel. Caries Res 39:380–386
13. ten Cate JM, Buijs MJ, Miller CC, Exterkate RA (2008) Elevated fluoride products enhance remineralization of advanced enamel lesions. J Dent Res 87:943–947
14. Son HJ, Kim WC, Jun SH, Kim YS, Ju SW, Ahn JS (2010) Influence of dentin porcelain thickness on layered all-ceramic restoration color. J Dent 38(Suppl 2):e71–e77
15. Joiner A (2004) Tooth colour: a review of the literature. J Dent 32 (Suppl 1):3–12
16. Johnston WM (2009) Color measurement in dentistry. J Dent 37 (Suppl 1):e2–e6
17. Li Q, Xu BT, Li R, Yu H, Wang YN (2010) Quantitative evaluation of colour regression and mineral content change of bleached teeth. J Dent 38:253–260
18. Lim HN, Yu B, Lee YK (2010) Spectroradiometric and spectrophotometric translucency of ceramic materials. J Prosthet Dent 104:239–246
19. Lim HN, Yu B, Lim JI, Lee YK (2010) Correlations between spectroradiometric and spectrophotometric colors of all-ceramic materials. Dent Mater 26:1052–1058
20. Krikken JB, Zijp JR, Huysmans MC (2008) Monitoring dental erosion by colour measurement: an in vitro study. J Dent 36:731–735

21. Kleter GA (1998) Discoloration of dental carious lesions (a review). Arch Oral Biol 43:629–632
22. Matis BA, Wang Y, Eckert GJ, Cochran MA, Jiang T (2006) Extended bleaching of tetracycline-stained teeth: a 5-year study. Oper Dent 31:643–651
23. Pinto CF, Paes Leme AF, Cavalli V, Giannini M (2009) Effect of 10% carbamide peroxide bleaching on sound and artificial enamel carious lesions. Braz Dent J 20:48–53
24. Tschoppe P, Neumann K, Mueller J, Kielbassa AM (2009) Effect of fluoridated bleaching gels on the remineralization of predemineralized bovine enamel in vitro. J Dent 37:156–162
25. Cochrane NJ, Cai F, Huq NL, Burrow MF, Reynolds EC (2010) New approaches to enhanced remineralization of tooth enamel. J Dent Res 89:1187–1197
26. Vieira AE, Delbem AC, Sassaki KT, Rodrigues E, Cury JA, Cunha RF (2005) Fluoride dose response in pH-cycling models using bovine enamel. Caries Res 39:514–520
27. Rodrigues E, Delbem AC, Pedrini D, de Oliveira MS (2008) PH-cycling model to verify the efficacy of fluoride-releasing materials in enamel demineralization. Oper Dent 33:658–665
28. Kawasaki K, Ruben J, Tsuda H, Huysmans MC, Takagi O (2000) Relationship between mineral distributions in dentine lesions and subsequent remineralization in vitro. Caries Res 34:395–403
29. ten Cate JM, Exterkate RA, Buijs MJ (2006) The relative efficacy of fluoride toothpastes assessed with pH cycling. Caries Res 40:136–141
30. Douglas RD, Steinhauer TJ, Wee AG (2007) Intraoral determination of the tolerance of dentists for perceptibility and acceptability of shade mismatch. J Prosthet Dent 97:200–208
31. LeGeros RZ (1990) Chemical and crystallographic events in the caries process. J Dent Res 69 Spec No:567–574, discussion 634–566
32. Lippert F, Lynch RJ, Eckert GJ, Kelly SA, Hara AT, Zero DT (2011) In situ fluoride response of caries lesions with different mineral distributions at baseline. Caries Res 45:47–55
33. Tanaka T, Yagi N, Ohta T, Matsuo Y, Terada H, Kamasaka K, To-o K, Kometani T, Kuriki T (2010) Evaluation of the distribution and orientation of remineralized enamel crystallites in subsurface lesions by X-ray diffraction. Caries Res 44:253–259
34. Zantner C, Martus P, Kielbassa AM (2006) Clinical monitoring of the effect of fluorides on long-existing white spot lesions. Acta Odontol Scand 64:115–122